

Strongly interacting two photon random walk in an array of single atom beam splitters

Xinyuan Zheng^{1,*} and Edo Waks^{1,2,3,†}

¹*Department of Electrical and Computer Engineering and
Institute for Research in Electronics and Applied Physics,
University of Maryland, College Park, Maryland 20742, USA*

²*Joint Quantum Institute, University of Maryland,
College Park, Maryland 20742, USA*

³*Department of Physics, University of Maryland,
College Park, Maryland 20742, USA*

(Dated: January 28, 2022)

Abstract

Photonic quantum walk is a powerful tool for quantum simulation. However, most theoretical and experimental works related to this topic have implemented the random walks with linear optical elements, which lack photon-photon interactions. Here we propose a novel way to implement a photonic discrete time quantum walk with strong interactions using single atom beam splitters. We theoretically calculate the dynamics of the random walk for the case of two photons using quantum trajectory theory. We show that the photon correlation functions exhibit strong photon-photon interaction and that the statistical pattern of the quantum walk can be tuned by post-selecting the delay between photon detection events. Finally, we propose a practical realization of our random walk based on time-multiplexed synthetic dimensions. Our proposal has opened the door of a novel approach for photonic quantum simulation.

Photonics provides an efficient way to implement quantum walks, which play an important role in quantum simulation[1, 2] and quantum computation[3, 4]. Photonic quantum walks can be realized using beam splitters[5–8] or coupled waveguide arrays[9–11] to simulate a wide range of Hamiltonians and implement quantum computing algorithms[1–4]. In the linear optical regime, a two photon random walk can simulate the dynamics of non-interacting bosons, fermions or anyons[5–8]. But in order to study strongly-correlated many-body physics, strong nonlinearity at the single photon level is required.

Two photon quantum walks with strong photon-photon interaction can potentially be realized in both discrete and continuous time. In the microwave regime, coupled cavity arrays containing superconducting quantum emitters offer a continuous time Jaynes-cummings Hubbard Hamiltonian that can support two polariton bound states similar to the Bose-Hubbard Hamiltonian[12–14]. For the discrete time quantum walk, some phenomenological nonlinearities have been proposed and studied[15–17], but we still lack physical systems that realize these nonlinearities. A more realistic nonlinearity that has been demonstrated experimentally typically relies on light scattering on a two-level atom strongly coupled to a waveguide[18–23]. These systems act as single atom mirrors or beam splitters[24, 25], and can potentially replace linear beam splitters used in linear discrete time quantum walks. But leveraging these nonlinearities in a photonic random walk is largely unexplored, and the theoretical analysis of these systems remains extremely complex.

Here we propose a strongly interacting discrete-time photonic random walk using single-

atom beam splitters. To analyze the system, we develop a formalism based on quantum trajectory theory to derive a direct solution to the output statistics of the walk[26, 27]. We observed highly entangled two photon output states by investigating two photon correlation functions in certain pairs of output channels. Furthermore, by post-selecting different time delays between two photon detection events we can tune the walkers to exhibit either correlated or anti-correlated statistical pattern. Finally, we propose a practical realization of our random walk based on time-multiplexed synthetic dimensions[28–31]. Our proposal demonstrates a new approach for quantum simulation using photons.

Before introducing the strongly interacting random walk, we first review the linear optical approach which is illustrated in Figure 1a. This method uses a beam splitter array, also referred to as a quantum Galton board. In the illustration, both photons start at position 0. At each step, the linear beam splitters direct each photon to the left or right with equal probabilities, generating a quantum walk. The output statistics after N total steps are a result of interference from the many different paths the photons can take to reach their respective output ports. The linear quantum Galton board has been extensively analyzed and experimentally demonstrated[5, 6, 28]. Although the quantum Galton board in Figure 1a can exhibit complex multi-photon interference effects that may be useful for Boson sampling experiments[5–8, 32], it cannot generate strong multi-photon correlations inherent to strongly interacting systems.

In order to introduce nonlinear interactions into the random walk, we replace the linear beam splitters in Figure 1a with single atom beam splitters to form a nonlinear Galton board shown in Figure 1b. The source in the dashed box in Figure 1a is now replaced with a cavity at step 0, position 0 that feeds the two photons into the system. Similar to [6], the quantum Galton board in Figure 1b essentially represents a discrete time quantum walk in a 1D system shown in Figure 1c. Using this correspondence, the single atom beam splitters in Figure 1b-1c partitions the field according to the new input-output relations as shown in Figure 1d:

$$\begin{aligned}\hat{a}_{n,x,R,out} &= \hat{a}_{n,x,L,in} + \sqrt{2\gamma}\hat{\sigma}_{n,x} \\ \hat{a}_{n,x,L,out} &= \hat{a}_{n,x,R,in} + \sqrt{2\gamma}\hat{\sigma}_{n,x}\end{aligned}\tag{1}$$

In the above equations, $\hat{\sigma}_{n,x}$ is the lowering operator for a two level atom at step n, position x, and $\hat{a}_{n,x,L/R,in/out}$ is the input/output operator in the left/right direction for the two level

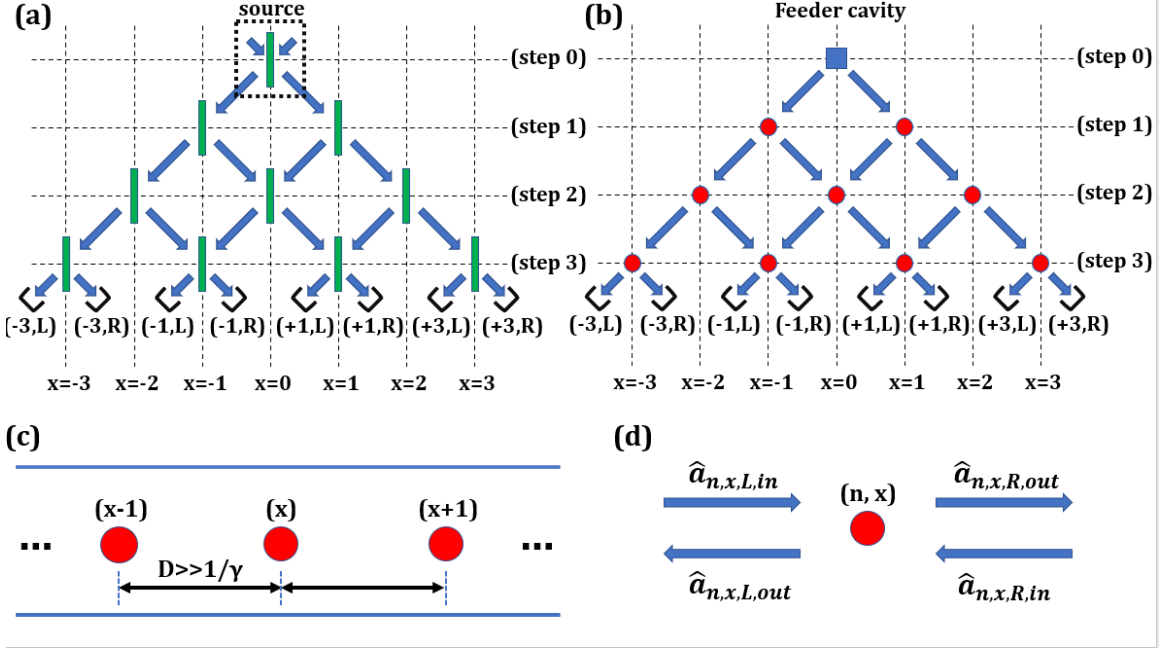


FIG. 1. (a) The common way to construct a two photon quantum walk with linear beam splitters. The source at step 0, $x=0$ injects a two photon state into the Galton board. The two photon state then undergoes 3 scattering events (i.e. 3 steps) before being detected at the detectors labeled from $(-3, L)$ to $(+3, R)$; (b) The nonlinear Galton board composed of a feeder cavity at step 0, $x = 0$. The linear beam splitters are replaced with single atom beam splitters and the source is now a feeder cavity; (c) An equivalent representation of the quantum walk. Note that each layer in (b) is a copy of the 1D system in (c) at a different time step. Also, the distance D between atoms in (c) should be much larger than the photon pulse width $\sim 1/\gamma$; (d) The input-output relation for each single atom beam splitter.

atom. For a single monochromatic photon, the single atom beam splitter behaves as a linear beam splitter [18, 25]. The reflection and transmission coefficients are given by $r_\delta = \frac{-i\gamma}{i\gamma + \delta}$ and $t_\delta = \frac{\delta}{i\gamma + \delta}$ [18], where $\Gamma_0 = 2\gamma$ is the decay rate of the atom and δ is the detuning between the atom and photon. Hence, one may reproduce the output of the quantum Galton board in Figure 1a by choosing the detuning to be $\gamma = \delta$. However, the single atom beam splitter exhibits a strong nonlinearity when more than one photon scatter on the same atom. To be precise, the two photon scattering can no longer be described by individual reflection and transmission coefficients. Instead, the atom mediates strong photon-photon interactions

giving rise to complex multi-photon scattering matrix elements[18–21].

Due to the strongly interacting nature of the nonlinear Galton board, the statistics of the detection events must be described by multi-photon correlation functions[33]. This work considers the special case of a two-photon random walk which is sufficiently tractable to be solved numerically. We initialize the feeder cavity to contain a two-photon Fock-state $|0, 0; 0, 0\rangle$, and allow the two photons to leak to the left or right with equal probability without any photon entanglement. The photons then undergo a sequence of N scattering events off the single atom beam splitters and finally generate photon counting events in the output channel detectors(Figure 1b). In this case, the statistics of the random walk are given by the two-photon correlation functions:

$$\Gamma_{x_2, d_2; x_1, d_1}(\tau, t) = |\langle vac | \hat{a}_{N, x_2, d_2, out}(t + \tau) \hat{a}_{N, x_1, d_1, out}(t) | 0, 0; 0, 0 \rangle|^2 \quad (2)$$

In the above equations, $|vac\rangle$ denotes the system ground state without any photon or excited atoms and $|0, 0; 0, 0\rangle = \frac{1}{\sqrt{2}}(\hat{b}_{0,0}^\dagger)^2 |vac\rangle$ is the initial state in which both photons are in the feeder cavity. Equation 2 then provides the time-ordered probability of collecting the first photon in detector $c_1 = (x_1, d_1)$ at time t and the second photon in detector $c_2 = (x_2, d_2)$ after some time interval $\tau \geq 0$.

Furthermore, to obtain more insight into the two photon interaction[33], we define the interval time correlation, $G_{c_1, c_2}(\tau) = \int_0^\infty dt \Gamma_{x_2, d_2; x_1, d_1}(\tau, t)$ which represents the marginal probability of detecting the photons separated by the time interval. The marginal probability retains the ordering of the arrival times of the two detectors. To average out over this time ordering we define the matrix $\tilde{G}_{c_1, c_2}(\tau) = G_{c_1, c_2}(\tau) + G_{c_2, c_1}(\tau)$ for all c_1, c_2 . We refer to this matrix as the statistical pattern. It shows the probabilities of the quantum walk after post-selecting all two photon detection events with a certain time interval τ regardless of time ordering. Conversely, we may also fix a pair of channels $c_1^{(0)}; c_2^{(0)}$ and plot both $G_{c_1^{(0)}; c_2^{(0)}}(\tau)$ and $G_{c_2^{(0)}; c_1^{(0)}}(\tau)$ for all $\tau \geq 0$. Such a curve reveals the distribution of the two output photons collected in $c_1^{(0)}; c_2^{(0)}$ with respect to their distance away from the center of mass.

To numerically calculate the correlation functions we use a quantum trajectory theory approach, originally proposed by Carmichael[26, 27] for the analysis of cascaded quantum systems. For the feeder cavity, the tunable decay rate κ and detuning δ allow us to control both the bandwidth and detuning of the input photons relative to the atomic transitions. All the atoms have decay rate γ . Following the quantum trajectory theory formalism,

we introduce the non-Hermitian Hamiltonian for the quantum Galton board given by (see supplementary section):

$$\begin{aligned}\hat{H} = & -2i(\kappa + i\delta)\hat{b}_{0,0}^\dagger\hat{b}_{0,0} - 2i\gamma \sum_{n,x} \hat{\sigma}_{n,x}^\dagger \hat{\sigma}_{n,x} \\ & - 2i\gamma \sum_{\substack{|n-n'|=|x-x'| \\ n>n', |x|\neq n}} \hat{\sigma}_{n,x}^\dagger \hat{\sigma}_{n',x'} - 2i\sqrt{\gamma\kappa} \sum_{n=1}^N (\hat{\sigma}_{n,-n}^\dagger + \hat{\sigma}_{n,n}^\dagger) \hat{b}_{0,0}\end{aligned}\quad (3)$$

where $1 \leq n \leq N$, $|x| \leq n$ and $x \equiv n(\text{mod}2)$ for any n, x . In the above Hamiltonian, $\hat{b}_{0,0}^\dagger$ is the raising operator for the feeder cavity and $\hat{\sigma}_{n,x}^\dagger$ is the raising operator of an atom at step n , position x . After N total steps, the output operator $\hat{a}_{N,x,d,out}$ in Equation 2 are related to the internal modes of the Hamiltonian by repeatedly applying Equation 1 (see supplementary section), yielding:

$$\begin{aligned}\hat{a}_{N,-N,L,out} &= \sqrt{2\kappa}\hat{b}_{0,0} + \sum_{1 \leq n' \leq N}^{x'=-n'} \sqrt{2\gamma}\hat{\sigma}_{n',x'} \\ \hat{a}_{N,N,R,out} &= \sqrt{2\kappa}\hat{b}_{0,0} + \sum_{1 \leq n' \leq N}^{x'=n'} \sqrt{2\gamma}\hat{\sigma}_{n',x'} \\ \hat{a}_{N,x,L,out} &= \sum_{n' \leq N}^{x'-x=N-n'} \sqrt{2\gamma}\hat{\sigma}_{n',x'} \quad (|x| \neq N) \\ \hat{a}_{N,x,R,out} &= \sum_{n' \leq N}^{x'-x=n'-N} \sqrt{2\gamma}\hat{\sigma}_{n',x'} \quad (|x| \neq N)\end{aligned}\quad (4)$$

Using Equation 3-4, we can then calculate all the two-photon correlations in Equation 2. The complete solving procedure is detailed in the supplementary section.

It should be noted that, even for a single photon random walk, the nonlinear galton board in Figure 1b and its linear counterpart in Figure 1a differ in an important way. Unlike the dispersionless linear beam splitters in Figure 1a, the single atom beam splitter has a highly dispersive splitting ratio even for one photon[18]. To accurately extract the effects of nonlinearity, we must compare the nonlinear Galton board to a linear Galton board that exhibits the same dispersion properties. To achieve this, we replace the beam splitters with linear cavities with the same resonant frequencies and decay rates as the single atom beam splitters (see supplementary section). Unlike the atom, the cavity does not induce two photon interaction but still has the same dispersion relation for the transmission and reflection coefficient.

We first analyze the case where the single atoms act as nearly ideal 50/50 beam splitters for a single photon input. To achieve this condition, we set $\gamma = \delta = 1$, and select the feeder cavity decay rate to be $\kappa = 0.005$. This decay rate is sufficiently small to ensure that the photon bandwidth is narrow compared to the atomic transition linewidth such that we are in the quasi-monochromatic limit. Figure 2a shows the statistical pattern after 9 steps for $\tau = 0$. The statistical pattern exhibits a strongly correlated behavior in which the two walkers walk together and are found at the same location. For comparison, Figure 2b shows the results for the linear Galton board. Here there is no correlation between the positions of the walkers, and the two walkers equally partition themselves to the left $(-5, L)$ and right $(+5, R)$. The strong correlations in Figure 2a are therefore a result of the two photon interactions induced by the single atom beam splitter.

Figure 2c plots the statistical pattern for $\tau = 0.7$. In this case the random walk exhibits a drastically different behavior. Instead of being strongly correlated, the statistical pattern becomes anti-correlated where the two walkers are found on opposite sides of the nonlinear Galton board. By tuning τ we can therefore change the nature of the statistics to be either correlated or anti-correlated. We note that the statistical pattern of the linear Galton board is independent of τ (see supplementary section), so we may still compare Figure 2c to Figure 2b to determine the effect of the nonlinearity. Finally, Figure 2d shows the case for $\tau = 5.0$. Here, we post select photon detection events that are sufficiently separated in time such that we may treat them as scattering individually, hence we recover the statistical pattern for the linear Galton board in Figure 2b.

To attain a better understanding of the varying statistical patterns, we select two representative channel pairs, as pointed out in Figure 2a, and plot the correlation $G_{c_1; c_2}(\tau)$ for all τ . For the the anti-correlated channels $(c_1; c_2) \in \{(-5, L; +5, R), (+5, R; -5, L)\}$ as shown in Figure 2e, we observe an oscillation in $G_{c_1; c_2}(\tau)$ that gradually dies out for $\tau > 6$. For the channel pair $(c_1; c_2) = (-5, L; -5, L)$ on the correlated diagonal, we observe a narrow peak around $\tau = 0$, followed by a valley with minimal value at $\tau = 0.7$ (Figure 2f). In comparison, for the linear Galton board, the correlation function $G_{c_1; c_2}(\tau)$ exhibits two identical smooth curves shown in blue (Figure 2e-2f), indicating no photon-photon interaction.

The nonlinear Galton board can also generate random walks with unequal splitting ratios by simply changing the detuning δ . As an instructive example, we analyze the case where the input photons are resonant with the single atom beam splitters ($\delta = 0$). In this regime

the device becomes a single atom *mirror* that reflects light with nearly unity efficiency[18]. Figure 3a shows the statistical pattern for $\tau = 0$, while Figure 3b shows the result for the linear random walk. For the linear random walk, the photons become trapped at the center. This behavior is expected because the photons repeatedly reflect back and forth from adjacent mirrors. Surprisingly, the nonlinear Galton board exhibits a statistical pattern that predominantly excludes the center region(Figure 3a). The photons escape the center and exhibit anti-correlated behavior where they are statistically most likely to be found at opposite ends of the Galton board. At $\tau = 1.5$ (Figure 3c) this anti-correlated statistical pattern gradually shrinks, while at $\tau = 5.0$ it becomes almost identical to the linear walk(Figure 3d).

Similarly, we pick two pairs of representative output channels indicated in Figure 3a and plot the correlation functions for all τ . For the nonlinear quantum walk, the correlation function in the anti-correlated channel pair $(-5, L; +5, R)$, $(+5, R; -5, L)$ as shown in Figure 3e reveals a high peak around $\tau = 0$ which indicates attractive photons. For other channel pairs on the anti-correlated diagonal excluding the center, similar two photon correlation functions can be observed(see supplementary section). In the center channel pair $(-1, R; +1, L)$, $(+1, L; -1, R)$ (Figure 3f), the photon correlation function exhibits a deep valley with minimum 0 around $\tau = 0$. Such a correlation function implies repulsive photon pairs in which the two photons are more likely to be found away from their center of mass.

Having analyzed the properties of the nonlinear Galton board, we next consider potential experimental realizations. The nonlinear Galton board illustrated in Figure 1b is beyond current experimental capabilities because it requires large arrays of identical nonlinear elements. To eliminate the need for large repeatable arrays of atoms, we consider an implementation of the nonlinear quantum Galton board using time multiplexed synthetic dimensions[28]. Figure 4a shows a conventional way of implementing a linear quantum walk in Figure 1a with only one beam splitter coupled to two feedback loops with different time delays. Such an implementation of the random walk has already been realized experimentally[28]. Essentially, the same linear beam splitter at different time bins $nT_0 + xT_x$ acts as the different beam splitters in the Galton board in Figure 1a, as long as the pulse width d of the photons satisfies $d \ll v_g T_x$ and $T_x \ll T_0$.

In order to transform the linear quantum random walk into a nonlinear random walk, we simply replace the linear beam splitter with a single atom beam splitter. The single atom beam splitter should be chirally coupled to the upper loop and the lower loop. We propose

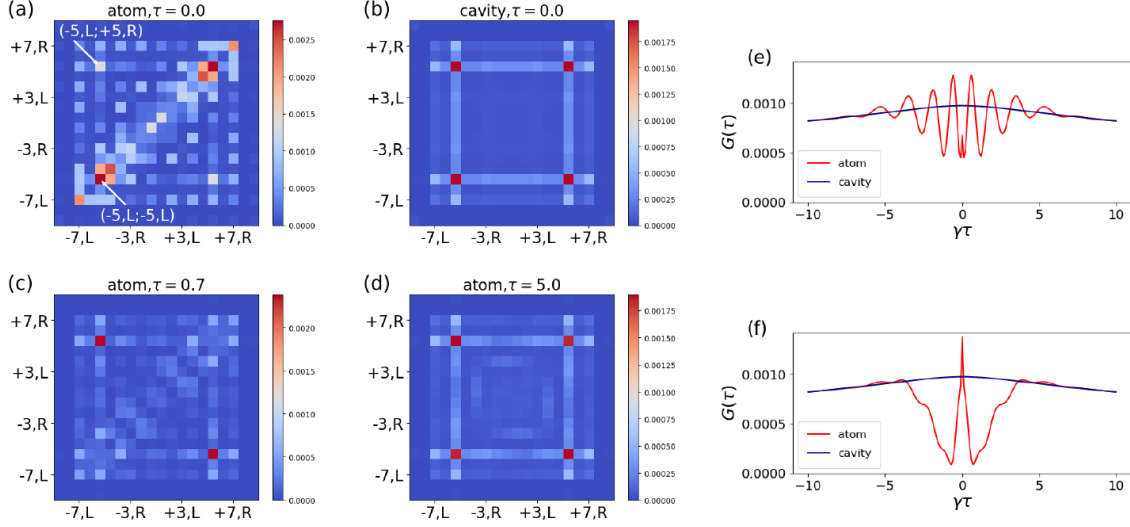


FIG. 2. Results for $\kappa \ll \delta = \gamma$. (a) The statistical pattern $\tilde{G}_{c_1;c_2}$ for the nonlinear Galton board when post-selecting detection events with time interval $\tau = 0$, showing correlated statistics; (b) The statistical pattern at $\tau = 0$ for the reference linear Galton board with the same dispersion relation; (c-d) The statistical pattern for the nonlinear Galton board at $\tau = 0.7, 5.0$, showing anti-correlated and uncorrelated statistics; (e) $G_{-5,L;+5,R}(\tau)$ and $G_{+5,R;-5,L}(-\tau)$, plotted for all $\tau \geq 0$; (f) $G_{-5,L;-5,L}(|\tau|)$ for all $\tau \geq 0$.

the setup in Figure 4b to satisfy this requirement and also achieve strong light-matter coupling. The atom (red) is first coupled chirally to a mode \hat{a}_r of a ring resonator (orange), which is then coupled to the two feedback loops modes \hat{a}_{up} and \hat{a}_{down} . As in [33], in the bad cavity limit, one can adiabatically eliminate the ring resonator degree of freedom and hence the atom is chirally coupled to the two modes \hat{a}_{up} and \hat{a}_{down} . This chirally coupled atom-cavity system has already been experimentally demonstrated [34] and the use of synthetic dimensions enables us to use existing technology to implement the nonlinear Galton board.

In summary, we have systematically studied a strongly interacting two photon quantum walk with single atom beam splitters and demonstrate the effect of nonlinearity by studying the correlation functions. Our quantum walk model can be easily generalized to more complicated quantum walks in high dimensions or with a gauge field [35] for more complicated quantum simulation tasks. Moreover, our model serves as a representative of a large family of light propagation problems consisting of one-way feed forward networks with nonlinear input-

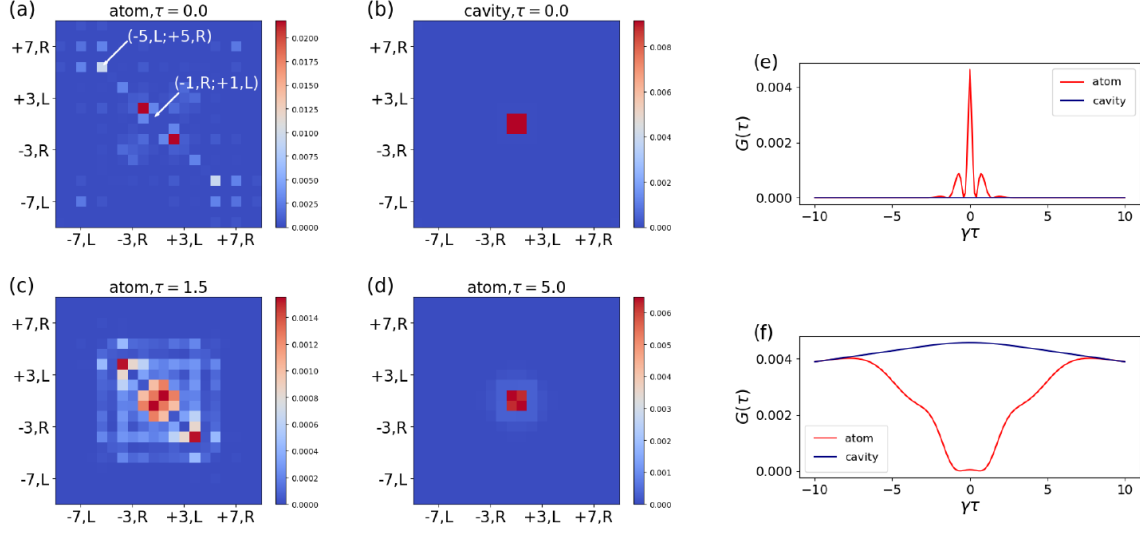


FIG. 3. Results for $\delta = 0$, $\kappa \ll \gamma$. (a) The statistical pattern $\tilde{G}_{c_1;c_2}$ for the nonlinear Galton board when post-selecting detection events with time interval $\tau = 0$, showing anti-correlated statistics excluding the center; (b) The statistical pattern at $\tau = 0$ for the reference linear Galton board; (c-d) The statistical pattern for the nonlinear Galton board at $\tau = 1.5, 5.0$. The statistical pattern for the nonlinear Galton board converges to the pattern in (b) as τ increases; (e) $G_{-5,L;+5,R}(\tau)$ and $G_{+5,R;-5,L}(-\tau)$, plotted for all $\tau \geq 0$; (f) $G_{-1,R;+1,L}(\tau)$ and $G_{+1,L;-1,R}(-\tau)$ for all $\tau \geq 0$.

output nodes. This broad family may include the classical n-photon scattering problem[18] or quantum neural networks[36]. Ultimately, our work can be extended in many ways and opens the door of a whole class of models with strong light-matter interaction for quantum simulation.

The authors would like to acknowledge financial support from the National Science Foundation (grant number OMA1936314 and ECCS1933546), the Air Force Office of Scientific Research (grant number UWSC12985 and FA23862014072), and the Army Research Laboratory (grant W911NF1920181).

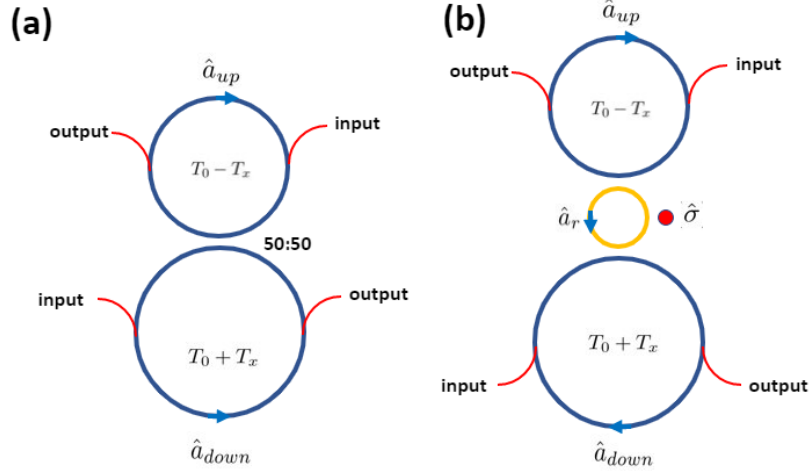


FIG. 4. (a) Implementing a quantum walk with linear 50/50 beam splitters using time-multiplexed synthetic dimensions; (b) Constructing a nonlinear quantum walk by replacing the 50/50 beam splitter with a single atom beam splitter. The single atom beam splitter consists of a two level atom (red) chirally coupled to the \hat{a}_r mode of a ring resonator (orange).

* xzheng16@terpmail.umd.edu

† edowaks@umd.edu

- [1] A. M. Childs, R. Cleve, E. Deotto, E. Farhi, S. Gutmann, and D. A. Spielman, Exponential algorithmic speedup by a quantum walk, in *Conference Proceedings of the Annual ACM Symposium on Theory of Computing* (2003) pp. 59–68.
- [2] A. M. Childs, D. Gosset, and Z. Webb, Universal computation by multiparticle quantum walk, *Science* **339**, 791 (2013), [arXiv:1205.3782](https://arxiv.org/abs/1205.3782).
- [3] J. Kempe, Quantum random walks: An introductory overview, *Contemporary Physics* **44**, 307 (2003), [arXiv:0303081](https://arxiv.org/abs/0303081) [quant-ph].
- [4] N. Shenvi, J. Kempe, and K. B. Whaley, Quantum random-walk search algorithm, *Physical Review A - Atomic, Molecular, and Optical Physics* **67**, 523071 (2003), [arXiv:0210064](https://arxiv.org/abs/0210064) [quant-ph].
- [5] F. De Nicola, L. Sansoni, A. Crespi, R. Ramponi, R. Osellame, V. Giovannetti, R. Fazio, P. Mataloni, and F. Sciarrino, Quantum simulation of bosonic-fermionic noninteracting parti-

- cles in disordered systems via a quantum walk, [Physical Review A - Atomic, Molecular, and Optical Physics](#) **89**, 32322 (2014), [arXiv:1312.5538](#).
- [6] L. Sansoni, F. Sciarrino, G. Vallone, P. Mataloni, A. Crespi, R. Ramponi, R. Osellame, F. De Nicola, L. Sansoni, A. Crespi, R. Ramponi, R. Osellame, V. Giovannetti, R. Fazio, P. Mataloni, and F. Sciarrino, Two-particle bosonic-fermionic quantum walk via integrated photonics, [Physical Review Letters](#) **108**, 1 (2012), [arXiv:1106.5713](#).
- [7] M. A. Broome, A. Fedrizzi, B. P. Lanyon, I. Kassal, A. Aspuru-Guzik, and A. G. White, Discrete single-photon quantum walks with tunable decoherence, [Physical Review Letters](#) **104**, 1 (2010), [arXiv:1002.4923](#).
- [8] T. Kitagawa, M. A. Broome, A. Fedrizzi, M. S. Rudner, E. Berg, I. Kassal, A. Aspuru-Guzik, E. Demler, and A. G. White, Observation of topologically protected bound states in photonic quantum walks, [Nature Communications](#) **3**, [10.1038/ncomms1872](#) (2012).
- [9] K. Poullos, R. Keil, D. Fry, J. D. Meinecke, J. C. Matthews, A. Politi, M. Lobino, M. Gräfe, M. Heinrich, S. Nolte, A. Szameit, and J. L. O'Brien, Quantum walks of correlated photon pairs in two-dimensional waveguide arrays, [Physical Review Letters](#) **112**, 1 (2014), [arXiv:1308.2554](#).
- [10] H. Tang, C. Di Franco, Z. Y. Shi, T. S. He, Z. Feng, J. Gao, K. Sun, Z. M. Li, Z. Q. Jiao, T. Y. Wang, M. S. Kim, and X. M. Jin, Experimental quantum fast hitting on hexagonal graphs, [Nature Photonics](#) **12**, 754 (2018), [arXiv:1807.06625](#).
- [11] H. Tang, X. F. Lin, Z. Feng, J. Y. Chen, J. Gao, K. Sun, C. Y. Wang, P. C. Lai, X. Y. Xu, Y. Wang, L. F. Qiao, A. L. Yang, and X. M. Jin, Experimental two-dimensional quantum walk on a photonic chip, [Science Advances](#) **4**, 1 (2018), [arXiv:1704.08242](#).
- [12] A. A. Houck, H. E. Türeci, and J. Koch, On-chip quantum simulation with superconducting circuits, [Nature Physics](#) **8**, 292 (2012).
- [13] Z. Yan, Y. R. Zhang, M. Gong, Y. Wu, Y. Zheng, S. Li, C. Wang, F. Liang, J. Lin, Y. Xu, C. Guo, L. Sun, C. Z. Peng, K. Xia, H. Deng, H. Rong, J. Q. You, F. Nori, H. Fan, X. Zhu, and J. W. Pan, [Strongly correlated quantum walks with a 12-qubit superconducting processor](#) (2019).
- [14] M. T. Wong and C. K. Law, Two-polariton bound states in the Jaynes-Cummings-Hubbard model, [Physical Review A - Atomic, Molecular, and Optical Physics](#) **83**, 1 (2011).
- [15] X. Y. Sun, Q. H. Wang, and Z. J. Li, Interacting Two-Particle Discrete-Time Quantum Walk with Percolation, [International Journal of Theoretical Physics](#) **57**, 2485 (2018).

- [16] S. D. Berry and J. B. Wang, Two-particle quantum walks: Entanglement and graph isomorphism testing, [Physical Review A - Atomic, Molecular, and Optical Physics](#) **83**, 1 (2011).
- [17] A. Bisio, G. M. D'Ariano, N. Mosco, P. Perinotti, and A. Tosini, Solutions of a two-particle interacting quantum walk, [Entropy](#) **20**, 10.3390/e20060435 (2018), [arXiv:1804.08508](#).
- [18] J. T. Shen and S. Fan, Strongly correlated multiparticle transport in one dimension through a quantum impurity, [Physical Review A - Atomic, Molecular, and Optical Physics](#) **76**, 10.1103/PhysRevA.76.062709 (2007).
- [19] Y. Shen and J. T. Shen, Photonic-Fock-state scattering in a waveguide-QED system and their correlation functions, [Physical Review A - Atomic, Molecular, and Optical Physics](#) **92**, 1 (2015).
- [20] S. Xu, E. Rephaeli, and S. Fan, Analytic properties of two-photon scattering matrix in integrated quantum systems determined by the cluster decomposition principle, [Physical Review Letters](#) **111**, 1 (2013).
- [21] S. Xu and S. Fan, Input-output formalism for few-photon transport: A systematic treatment beyond two photons, [Physical Review A - Atomic, Molecular, and Optical Physics](#) **91**, 1 (2015), [arXiv:1502.06049](#).
- [22] O. Firstenberg, T. Peyronel, Q. Y. Liang, A. V. Gorshkov, M. D. Lukin, and V. Vuletić, Attractive photons in a quantum nonlinear medium, [Nature](#) **502**, 71 (2013).
- [23] Q. Y. Liang, A. V. Venkatramani, S. H. Cantu, T. L. Nicholson, M. J. Gullans, A. V. Gorshkov, J. D. Thompson, C. Chin, M. D. Lukin, and V. Vuletić, Observation of three-photon bound States in a quantum nonlinear medium, [Science](#) **359**, 783 (2018), [arXiv:1709.01478](#).
- [24] S. Mahmoodian, G. Calajó, D. E. Chang, K. Hammerer, and A. S. Sørensen, Dynamics of Many-Body Photon Bound States in Chiral Waveguide QED, [Physical Review X](#) **10**, 31011 (2020), [arXiv:1910.05828](#).
- [25] D. E. Chang, L. Jiang, A. V. Gorshkov, and H. J. Kimble, Cavity QED with atomic mirrors, [New Journal of Physics](#) **14**, 10.1088/1367-2630/14/6/063003 (2012), [arXiv:1201.0643](#).
- [26] H. Carmichael, *An Open Systems Approach to Quantum Optics*, *Lecture Notes in Physics m18* (1991) p. 147, [arXiv:1211.6245](#).
- [27] H. J. Carmichael, Quantum trajectory theory for cascaded open systems, [Physical Review Letters](#) **70**, 2273 (1993).
- [28] A. Schreiber, K. N. Cassemiro, V. Potoček, A. Gábris, P. J. Mosley, E. Andersson, I. Jex, and

- C. Silberhorn, Photons walking the line: A quantum walk with adjustable coin operations, *Physical Review Letters* **104**, 1 (2010), [arXiv:0910.2197](#).
- [29] A. Schreiber, K. N. Cassemiro, V. Potoček, A. Gábris, I. Jex, and C. H. Silberhorn, Decoherence and disorder in quantum walks: From ballistic spread to localization, *Physical Review Letters* **106**, 1 (2011), [arXiv:1101.2638](#).
- [30] A. Schreiber, A. Gábris, P. P. Rohde, K. Laiho, M. Štefaňák, V. Potoček, C. Hamilton, I. Jex, and C. Silberhorn, A 2D quantum walk simulation of two-particle dynamics, *Science* **335**, 55 (2012), [arXiv:1204.3555](#).
- [31] T. Nitsche, F. Elster, J. Novotný, A. Gábris, I. Jex, S. Barkhofen, and C. Silberhorn, Quantum walks with dynamical control: Graph engineering, initial state preparation and state transfer, *New Journal of Physics* **18**, 10.1088/1367-2630/18/6/063017 (2016), [arXiv:1601.08204](#).
- [32] Y. Shikano, T. Wada, and J. Horikawa, Discrete-time quantum walk with feed-forward quantum coin, *Scientific Reports* **4**, 1 (2014).
- [33] S. Rosenblum, S. Parkins, and B. Dayan, Photon routing in cavity QED: Beyond the fundamental limit of photon blockade, *Physical Review A - Atomic, Molecular, and Optical Physics* **84**, 1 (2011), [arXiv:1109.1197](#).
- [34] B. Dayan, a. S. Parkins, T. Aoki, E. P. Ostby, K. J. Vahala, and H. J. Kimble, A Photon Turnstile Dynamically Regulated by One Atom, *Science* **319**, 22 (2008).
- [35] H. Chalabi, S. Barik, S. Mittal, T. E. Murphy, M. Hafezi, and E. Waks, Synthetic Gauge Field for Two-Dimensional Time-Multiplexed Quantum Random Walks, *Physical Review Letters* **123**, 150503 (2019).
- [36] G. R. Steinbrecher, J. P. Olson, D. Englund, and J. Carolan, Quantum optical neural networks, *npj Quantum Information* **5**, 1 (2019), [arXiv:1808.10047](#).

Supplementary Information: Strongly interacting two photon random walk in an array of single atom beamsplitters

I. METHOD AND FORMALISM

I.1. Derivation of input/output operators

We first derive the input/output operator at step n for arbitrary $n \leq N$ where N is the total number of steps. For a Galton board as shown below, we first define the following functions for site (n_1, x_1) and (n_2, x_2) :

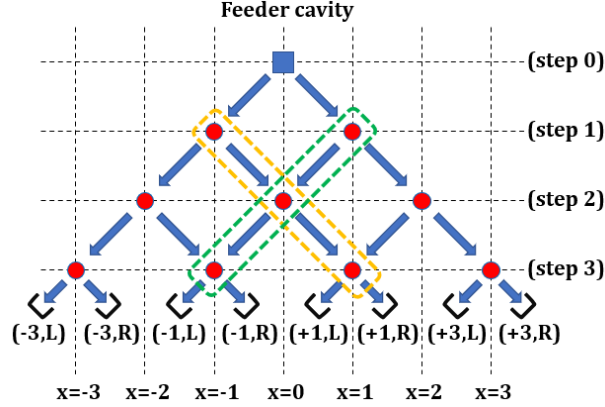


FIG. S1: A nonlinear Galton board with 3 steps. As an example, each pair of atoms in the green dashed box with $n_1 \neq n_2$ satisfies $\text{inline}(n_1, x_1; n_2, x_2) = -1$ whereas each pair in the orange dashed box with $n_1 \neq n_2$ satisfies $\text{inline}(n_1, x_1; n_2, x_2) = +1$.

$$\begin{aligned}
 \text{valid}(n_1, x_1) &= \begin{cases} 1, & \text{if } x_1 \equiv n_1 \pmod{2} \text{ and } |x_1| \leq n_1 \\ 0, & \text{else} \end{cases} \\
 \text{order}(n_1, x_1) &= n_1(n_1 + 1) + x_1 \\
 \text{inline}(n_1, x_1; n_2, x_2) &= \begin{cases} 1, & \text{if } n_1 - n_2 = x_1 - x_2, n_1 \neq n_2 \\ 0, & \text{else} \\ -1, & \text{if } n_1 - n_2 = x_2 - x_1, n_1 \neq n_2 \end{cases} \\
 \text{ift}(n_1, x_1; n_2, x_2) &= \begin{cases} 2, & \text{if } n_1 = x_1 = n_2 = x_2 = 0 \\ 1, & \text{else} \end{cases}
 \end{aligned} \tag{S1}$$

Intuitively, (n_1, x_1) is valid if such a site exist in a Galton board shown in (e.g. $(1, -1)$ is valid but $(1, 0)$ is not). Any pair of labels (n, x) appearing in the equations below should satisfy $\text{valid}(n, x) = 1$. The order function labels the sites with unique integers from step 0 to step N . The inline function determines whether two sites are in the same line. Note that it yields $+1$ if (n_1, x_1) is on the top left of (n_2, x_2) and -1 otherwise, as shown in Figure S1. For simplicity, we define site operator $\hat{s}_{0,0} = \hat{b}_{0,0}$ and $\hat{s}_{n \neq 0, x} = \hat{\sigma}_{n, x}$. Similarly, the decay rate for each site is defined as $dr_{0,0} = \kappa$ and $dr_{n \neq 0, x} = \gamma$ where κ, γ are the decay rates of the cavity and atom, respectively. The ift function is introduced since $\hat{s}_{0,0}$ is bosonic, i.e. $|0, 0; 0, 0\rangle = \frac{1}{\sqrt{2}}(\hat{s}_{0,0}^\dagger)^2 |vac\rangle$. We can thus generally write

$$|n_1, x_1; n_2, x_2\rangle = \frac{1}{\sqrt{\text{ift}(n_1, x_1; n_2, x_2)}} \hat{s}_{n_1, x_1}^\dagger \hat{s}_{n_2, x_2}^\dagger |vac\rangle$$

Now we derive the input/output operator for arbitrary valid site (n_1, x_1) . The input/output relations can now be written as:

$$\begin{aligned}
 \hat{a}_{n, x, L, out} &= \hat{a}_{n, x, R, in} + \sqrt{2dr_{n, x}} \hat{s}_{n, x} \\
 \hat{a}_{n, x, R, out} &= \hat{a}_{n, x, L, in} + \sqrt{2dr_{n, x}} \hat{s}_{n, x}
 \end{aligned} \tag{S2}$$

For all (n, x) such that $|n| = |x|$, we have the boundary condition:

$$\begin{aligned} \hat{a}_{0,0,L,in} &= \hat{a}_{0,0,R,in} = 0 \\ \hat{a}_{n,-n,L,in} &= \hat{a}_{n,n,R,in} = 0 \quad (\forall n \geq 1) \end{aligned} \quad (S3)$$

Without loss of generality, we have the additional relations:

$$\begin{aligned} \hat{a}_{n,x,L,out} &= \hat{a}_{n+1,x-1,R,in} \\ \hat{a}_{n,x,R,out} &= \hat{a}_{n+1,x+1,L,in} \end{aligned} \quad (S4)$$

By plugging in Equation S1 \sim S4, an arbitrary input/output operator can be written as:

$$\begin{aligned} \hat{a}_{n,x,L,in} &= \sum_{\substack{order(n',x') < order(n,x) \\ inline(n',x';n,x)=1}} \sqrt{2dr_{n',x'}} \hat{s}_{n',x'} \\ \hat{a}_{n,x,R,in} &= \sum_{\substack{order(n',x') < order(n,x) \\ inline(n',x';n,x)=-1}} \sqrt{2dr_{n',x'}} \hat{s}_{n',x'} \\ \hat{a}_{n,x,R,out} &= \sqrt{2dr_{n,x}} \hat{s}_{n,x} + \sum_{\substack{order(n',x') < order(n,x) \\ inline(n',x';n,x)=1}} \sqrt{2dr_{n',x'}} \hat{s}_{n',x'} \\ \hat{a}_{n,x,L,out} &= \sqrt{2dr_{n,x}} \hat{s}_{n,x} + \sum_{\substack{order(n',x') < order(n,x) \\ inline(n',x';n,x)=-1}} \sqrt{2dr_{n',x'}} \hat{s}_{n',x'} \end{aligned} \quad (S5)$$

By plugging in $\hat{s}_{n,x}$ and $dr_{n,x}$, we get equation (4) in the manuscript as desired.

I.2. The effective Hamiltonian

Here we will use the result in section I.1 to find the effective Hamiltonian[1, 2]. We do this by induction, as shown in Figure S2.

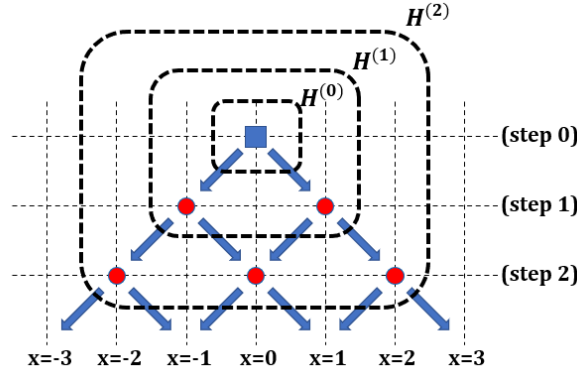


FIG. S2: $H^{(0)}$, $H^{(1)}$ and $H^{(2)}$ for a quantum Galton board.

In general, the Hamiltonian of the $n \geq 0$ step Galton board (i.e. $H^{(n)}$) drives the atoms at step $n+1$ with corresponding output operators, forming $H^{(n+1)}$. The case of $n = 0, 1, 2$ are shown in Figure S2. For $n = 0$, we get $H^{(0)} = -2i(\kappa + i\delta)\hat{b}_{0,0}^\dagger\hat{b}_{0,0}$ where κ is the feeder cavity decay rate and δ is the relative detuning between the feeder cavity and the atom. For any $n \geq 1$, we have:

$$H^{(n)} = H^{(n-1)} - i \sum_x \sqrt{2dr_{n,x}} \hat{s}_{n,x}^\dagger (\hat{a}_{n,x,L,in} + \hat{a}_{n,x,R,in}) - 2i \sum_x dr_{n,x} \hat{s}_{n,x}^\dagger \hat{s}_{n,x} \quad (S6)$$

Hence, by applying the above formula for $n = 1, 2, \dots, N$, we get the Hamiltonian for a quantum walk with N total steps:

$$H^{(n)} = -2i(dr_{0,0} + i\delta)\hat{s}_{0,0}^\dagger\hat{s}_{0,0} - i \sum_{1 \leq n \leq N, x} \sqrt{2dr_{n,x}}\hat{s}_{n,x}^\dagger(\hat{a}_{n,x,L,in} + \hat{a}_{n,x,R,in}) - 2i \sum_{1 \leq n \leq N, x} dr_{n,x}\hat{s}_{n,x}^\dagger\hat{s}_{n,x} \quad (S7)$$

By plugging in S5, we get an alternative form:

$$H^{(n)} = -2i(dr_{0,0} + i\delta)\hat{s}_{0,0}^\dagger\hat{s}_{0,0} - 2i \sum_{\substack{order(1,-1) \leq order(n,x) \leq order(N,N) \\ |inline(n',x';n,x)|=1}} dr_{n,x}\hat{s}_{n,x}^\dagger\hat{s}_{n,x} - 2i \sum_{\substack{order(n',x') < order(n,x) \leq order(N,N)}} \sqrt{dr_{n',x'}dr_{n,x}}\hat{s}_{n,x}^\dagger\hat{s}_{n',x'} \quad (S8)$$

In summary, the Hamiltonian is a sum of terms of the form $-2i \times hc_{n',x';n,x}\hat{s}_{n,x}^\dagger\hat{s}_{n',x'}$ for $order(n,x) = order(n',x')$ or for $order(n',x') < order(n,x)$. The Hamiltonian coefficients $hc_{n',x';n,x}$ are given by $hc_{n',x';n,x} = \sqrt{dr_{n',x'}dr_{n,x}}$ except for $hc_{0,0;0,0} = \sqrt{dr_{0,0}dr_{0,0}} + i\delta$.

I.3. Solving the propagators

We are now ready to solve the dynamics of the system. Recall that in our quantum walk, the initial state of the system is $|0,0;0,0\rangle$. The system first evolves for time t according to the equation $i\frac{d}{dt}|\psi\rangle = H^{(N)}|\psi\rangle$ until one photon is detected at one of the output channels. The system then collapses into a one excitation state and evolves for another time interval τ before the second photon is detected and the system goes back to $|vac\rangle$. Hence, we define two photon propagator function $tpp_{n_1,x_1;n_2,x_2}(t)$ as follows:

$$tpp_{n_1,x_1;n_2,x_2}(t) = \langle n_1, x_1; n_2, x_2 | e^{-iH^{(N)}t} | 0, 0; 0, 0 \rangle \quad (S9)$$

And we require $order(n_1, x_1) \leq order(n_2, x_2)$ to avoid double counting. Hence, $tpp_{n_1,x_1;n_2,x_2}(t)$ represents the probability amplitude in front of the state vector $|n_1, x_1; n_2, x_2\rangle$ if we start with the initial state $|0, 0; 0, 0\rangle$ and evolve for time t .

We also need to define single photon propagator function $opp_{n_1,x_1;n_2,x_2}(\tau)$:

$$opp_{n_1,x_1;n_2,x_2}(\tau) = \langle n_2, x_2 | e^{-iH^{(N)}\tau} | n_1, x_1 \rangle \quad (S10)$$

Equivalently, $opp_{n_1,x_1;n_2,x_2}$ thus represents the probability amplitude, or complex value function in front of the basis vector $|n_2, x_2\rangle$ if we start with the initial state $|n_1, x_1\rangle$ and evolve it using the effective Hamiltonian for time τ .

We first demonstrate how to solve for all $opp_{n_1,x_1;n_2,x_2}(\tau)$. The differential equation for such propagator is:

$$\begin{aligned} \frac{d}{dt} opp_{n_1,x_1;n_2,x_2}(\tau) = & -(2hc_{n_2,x_2;n_2,x_2})opp_{n_1,x_1;n_2,x_2}(\tau) \\ & - \sum_{\substack{order(n_3,x_3) < order(n_2,x_2), inline(n_3,x_3;n_2,x_2)=\pm 1 \\ valid(n_3-n_1,x_3-x_1)=1}} (2hc_{n_3,x_3;n_2,x_2})opp_{n_1,x_1;n_3,x_3} \end{aligned} \quad (S11)$$

For example, the "bottom layer" opp $opp_{0,0;2,0}$ would depend on the "top layer" opps: $\{opp_{0,0;1,-1}, opp_{0,0;1,1}\}$. These two opps would further be deduced from $opp_{0,0;0,0} = e^{-(2\kappa+2i\delta)\tau}$. Likewise, $opp_{1,1;3,1}$ would depend on the set $\{opp_{1,1;2,0}, opp_{1,1;2,2}\}$. It should be noted that only $opp_{n_1,x_1;n_2,x_2}$ is non-zero only if (n_2, x_2) lies in the "light cone" of (n_1, x_1) as shown in Figure S3. Namely, we have $valid(n_2 - n_1, x_2 - x_1) = 1$.

From equation S11, one can see that $opp(n_1, x_1; n_1, x_1) = e^{-2hc_{n_1,x_1;n_1,x_1}\tau}$ and using induction, we can show that any opp has analytic solution of the form $F_1(t) = e^{-2\gamma\tau}p_1(\tau) + e^{-(2\kappa+2i\delta)\tau}p_2(\tau)$ where p_1, p_2 are some polynomials with finite order. We are then able to find the polynomial coefficients and hence the analytic solutions using induction.

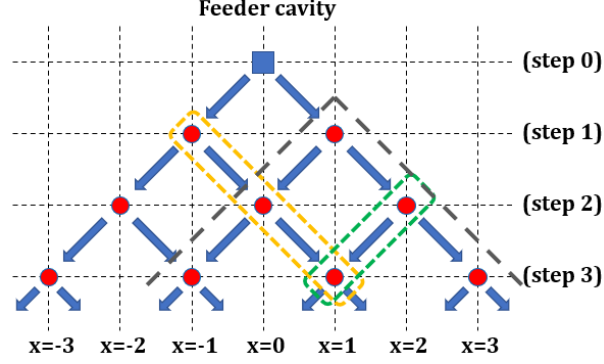


FIG. S3: The light cone in grey for site (1, 1). It should be notice that for site (3, 1), $opp_{1,1;3,1}$ would only rely on $opp_{1,1;n,x}$ for (n, x) in the light cone of (1, 1). Also, we must have $inline(n, x; 3, 1) = \pm 1$ and $order(n, x) < order(3, 1)$.

We now use two-photon version of the above method to find all tpps. The equation for a tpp is:

$$\begin{aligned}
 \frac{d}{dt} tpp_{n_1, x_1; n_2, x_2}(t) = & -(2hc_{n_1, x_1; n_1, x_1} + 2hc_{n_2, x_2; n_2, x_2}) tpp_{n_1, x_1; n_2, x_2}(t) \\
 & - \sum_{\substack{order(n_3, x_3) < order(n_1, x_1) \\ inline(n_3, x_3; n_1, x_1) = \pm 1}} (2hc_{n_3, x_3; n_1, x_1}) tpp_{n_3, x_3; n_2, x_2}(t) \\
 & - \sum_{\substack{order(n_1, x_1) < order(n_4, x_4) < order(n_2, x_2), inline(n_4, x_4; n_2, x_2) = \pm 1 \\ valid(n_3 - n_1, x_3 - x_1) = 1}} (2hc_{n_4, x_4; n_2, x_2}) tpp_{n_1, x_1; n_4, x_4}(t) \\
 & - \sum_{\substack{order(n_4, x_4) \leq order(n_1, x_1), inline(n_4, x_4; n_2, x_2) = \pm 1 \\ valid(n_3 - n_1, x_3 - x_1) = 1}} (2hc_{n_4, x_4; n_2, x_2}) tpp_{n_4, x_4; n_1, x_1}(t)
 \end{aligned} \tag{S12}$$

One can see that except for $(0, 0; 0, 0)$, $tpp_{n_1, x_1; n_2, x_2} = 0$ for all $(n_1, x_1) = (n_2, x_2)$. Using a similar argument, we find that all tpp has the form $F_2(t) = e^{-4\gamma t} q_1(t) + e^{-(2\kappa + 2i\delta + 2\gamma)t} q_2(t) + e^{-(4\kappa + 4i\delta)t} q_3(t)$. Again, q_1, q_2, q_3 are polynomials with finite order.

Again, we can recursively find the poynomial coefficients and hence the analytic solutions, starting from $tpp(0, 0; 0, 0) = e^{-(4\kappa + 4i\delta)t}$.

I.4. Computing correlations

Finally, we may obtain the correlations functions by combining opps with tpps. We start with the simpler correlations $\langle vac | \hat{s}_{n_2, x_2} e^{-iH\tau} \hat{s}_{n_1, x_1} e^{-iHt} | 0, 0; 0, 0 \rangle$, and note that:

$$\langle vac | \hat{s}_{n_1, x_1} e^{-iH\tau} \hat{s}_{n_2, x_2} e^{-iHt} | 0, 0; 0, 0 \rangle = \sum_{order(n_3, x_3) \leq order(n_2, x_2)} \sqrt{ift(n_3, x_3; n_2, x_2)} tpp(n_3, x_3; n_2, x_2) opp(n_3, x_3; n_1, x_1) \tag{S13}$$

Now the correlations we want are $\langle vac | \hat{a}_{1, out} e^{-iH\tau} \hat{a}_{2, out} e^{-iHt} | 0, 0; 0, 0 \rangle$ where $\hat{a}_{i, out}$ are output operators in equation S5 for $n = N$. These correlations are just linear combinations of the above correlations due to the relations in equation S5. Hence, we obtain the solution for all correlation functions.

I.5. A linear quantum walk model with dispersion

As mentioned in the main text, to accurately extract the effect of interactions, we need to consider a Galton board with the same dispersion relations in beam splitting ratio but with no photon-photon interaction. To achieve this, we simply replace all $\hat{\sigma}_{n,x}$ in equation S1 with bosonic operators $\hat{b}_{n,x}$. Namely, we replace the single atom beam splitters with linear cavity beam splitters with the same resonant frequency and decay rate. For a single

photon, this replacement makes no difference. However, for a two photon quantum walk, note that in general, $tpp(n_1, x_1; n_1, x_1) \neq 0$ for $(n_1, x_1) \neq (0, 0)$ since we no longer have Pauli exclusion principle for each site.

RESULTS

Case 1: $\gamma = \delta$

Here we present further results for $\kappa \ll \gamma = \delta$. In particular, we present the statistical patterns for the reference model (i.e. the non-interacting quantum walk with linear cavities). Indeed, as shown in Figure S4, the statistical pattern is τ -invariant.

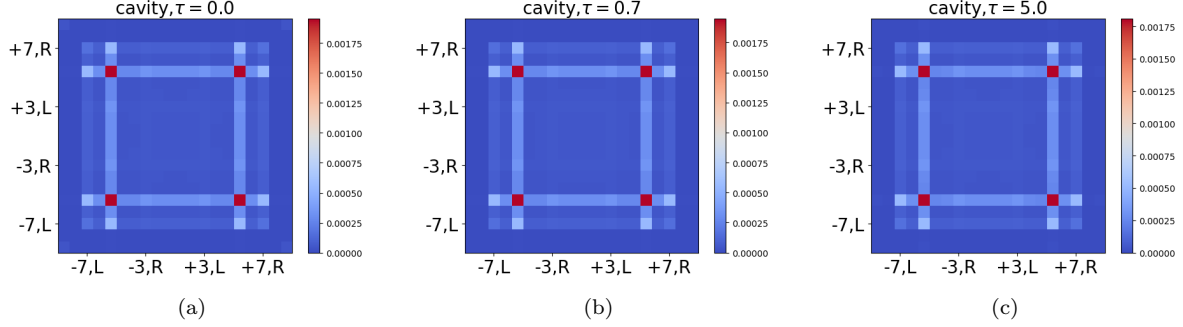


FIG. S4: τ -invariant statistical pattern of the linear quantum walk, for $\delta = \gamma$. For this set of parameters, the cavity act as a 50/50 beam splitter.

Case 2: $\delta = 0$

For the resonant case(Figure S5), we see once again that the statistical pattern for the linear cavity beamsplitter quantum walk is τ -invariant. Furthermore, we pick two extra pairs of channels on the anti-correlated diagonal $(-3, L; +3, R); (+3, R; -3, L)$ and $(-1, L; +1, R); (+1, R; -1, L)$ and compare the correlation function $G(\tau)$ for all τ for both the linear and nonlinear quantum walk(Figure S6). These two pairs of channels exhibits similar correlation functions to that of the channel pair $(-5, L; +5, R); (+5, R; -5, L)$.

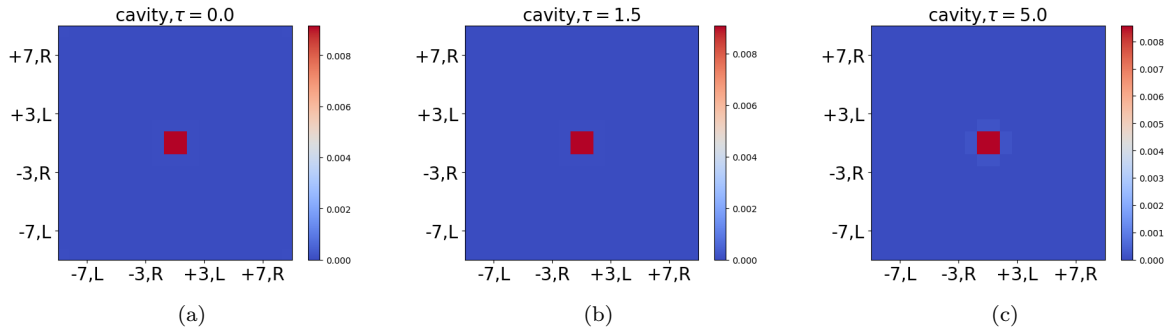


FIG. S5: τ -invariant statistical pattern of the linear quantum walk, for $\delta = 0$. For this set of parameters, the cavity act as a near perfect mirror.

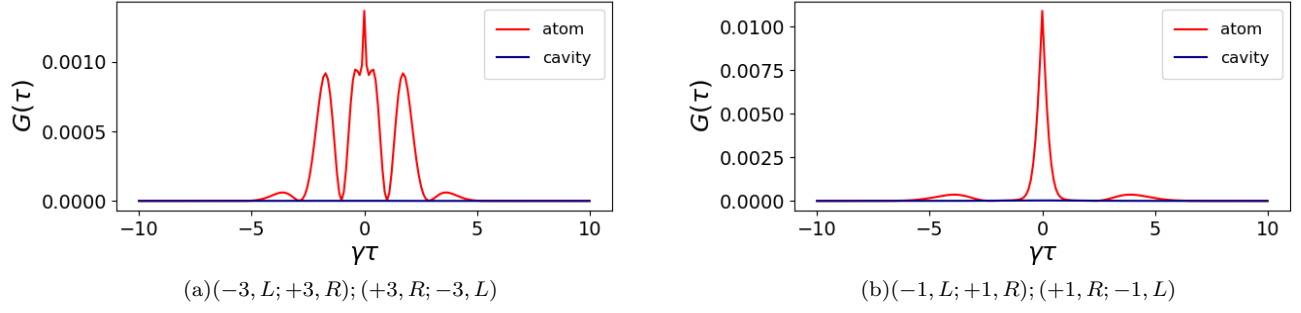


FIG. S6: Correlation function $G(\tau)$ for two pairs of output channels on the anti-correlated diagonal. Note that the nature of correlation is similar to that of the channel pair $(-5, L; +5, R); (+5, R; -5, L)$ shown in the main text.

-
- [1] H. Carmichael, *An Open Systems Approach to Quantum Optics, Lecture Notes in Physics m18* (1991), ISBN 3540566341, 1211.6245.
- [2] H. J. Carmichael, *Physical Review Letters* **70**, 2273 (1993), ISSN 00319007.